UNIVERSITY OF BIRMINGHAM

Investigation into Cavity Axis Shifts and Tilts Using the Finesse Modal Model

Mauricio D.Ortiz jr, Aaron W. Jones, Marie-Sophie Hartig,
Ali L. James, Luis Ortega

Issue: LIGO-T1900708-v3

Date: April 20, 2021

Finesse Workshop 2019
Hosted at: Institute for Gravitational Wave Astronomy and School of Physics and Astronomy
University of Birmingham
Birmingham, B15 2TT

Contents

1 Introduction **2**

2 Analytical Solution **2**

3 The Modal Model **4**

4 Finesse Model **4**

5 Comparison **6**

5.1 Spot Position Mismatches 7

5.2 Cavity Axis Mismatches 7

6 Conclusions **7**

1 Introduction

Suspended optical cavities are frequently used in precision measurements such as Gravitational Wave detection. In such optical cavities pitch and yaw motion of the mirrors with respect to the input laser can cause the axis on which the cavity resonates to shift. In this document we explore how to model these shifts and tilts using FINESSE (v 2.3.1), an interferometer modelling tool commonly used in the gravitational wave community.

The document is structured as follows: in Section 2 we highlight analytic equations which describe the cavity axis shift and tilt for a two mirror infinite finesse cavity; in section 3 we describe the modal model we use; in section 4 we outline a relationship between the finesse outputs and cavity axis shift and tilt, valid at any point in the resonator; and in section 5 we compare our anayltic solution against our finesse model in the case of a two mirror hemispherical cavity.

2 Analytical Solution

We look at the expected translation of a cavity axis using geometrical arguments. All formulas and how they arise originate from Siegman [4], chapter 19. In the following, the index for each variable indicates which optic we are referring to. Without any known loss of generality, we consider a hemispherical cavity. We define the length of the cavity L and the radii of curvature R_{M1} and R_{M2} of the mirrors M_1 and M_2. We chose the first mirror, M_1, to be flat, i.e. $R_{M1} = \infty$. The tilting angles are given by θ_1 and θ_2. They describe the rotations of the mirrors in a global coordinate system.

We define the resonator g-parameters as $g = 1 - \frac{L}{R}$, hence

$$g_1 = 1\,, \tag{1}$$

$$g_2 = 1 - \frac{L}{R_{M2}}\,. \tag{2}$$

The parameter g_2 becomes negative if $L > R_{M2}$. This is when the centre of the circle defined by the curved mirror surfaces sits between the two mirrors. If the investigated mirror is flat, R_{M2} becomes infinite and hence $\frac{L}{R_{M2}}$ is zero.

The translation of the cavity axis is shown in figure 1. It is derived the following way: We first examine the centres of the circles defined by the curved mirror surfaces. For the flat mirror this point is found to be infinitely far from the mirrors surface in the direction of its surface normal vector. In the next step we draw a line intersecting these two points. The height of the line at the mirrors defines the wanted translation. It is analytically given by

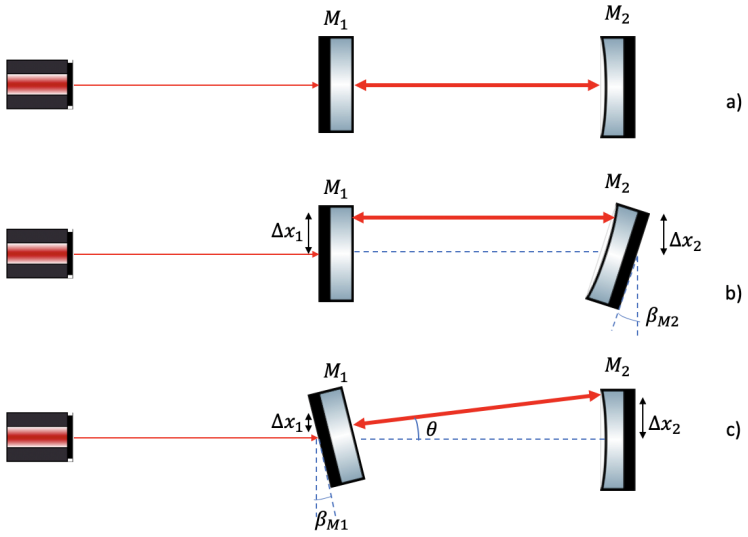

Figure 1: *Diagram showing the misalignment's modelled on Finesse. a) shows the initial setup with the cavity mirrors perfectly aligned. b) shows how the cavity eigenmode shifts parallel to the input axis as the curved mirror is rotated for a given angle β_{M2}. In this scenario the tilt of the eigenmode, $\theta = 0°$ such that the shift of the beam spot on each mirror is the same, $\Delta x_1 = \Delta x_2$. c) shows the resultant shift and tilt of the cavity eigenmode for a tilt of β_{M1}. Unless the flat mirror is placed at the radius of curvature of the curved mirror there will be a beam shift on the flat mirror.*

$$\Delta x_1 = \frac{g_2}{1 - g_1 \cdot g_2} L \cdot \theta_1 - \frac{1}{1 - g_1 \cdot g_2} L \cdot \theta_2 \,, \tag{3}$$

$$\Delta x_2 = \frac{1}{1 - g_1 \cdot g_2} L \cdot \theta_1 - \frac{g_1}{1 - g_1 \cdot g_2} L \cdot \theta_2 \,. \tag{4}$$

Note that the signs of the θ_2-dependent parts are chosen contrary to the sign in [4]. Investigating Figure 1 and rotating the mirrors in a global coordinate system, we find them to be negative.

Next to the translations we also analyse the angular displacement of the optical axis. Since we only assume small rotation angles, it is approximately given by,

$$\Delta\theta = \frac{\Delta x_1 - \Delta x_2}{L} \,. \tag{5}$$

3 The Modal Model

Under the paraxial approximation we can describe the light resonating in the optical cavity by a sum of higher order spatial modes[2],

$$E(t,x,y,z) = \sqrt{P}\sum_j \sum_{nm} a_{jnm} u_{nm}(x,y,z) \exp\left(i\left(\omega_j t - k_j z\right)\right). \tag{6}$$

We use the Hermite-Gauss modes and so for a anastigmatic beam the mode function is,

$$\begin{aligned} u_{nm}(x,y,z) =& \sqrt{\frac{1}{2^{n+m-1} n! m! \pi}} \frac{1}{w(z)} \exp\left(i\left(n+m+1\right)\Psi(z)\right) \\ & H_n\left(\frac{\sqrt{(}2)x}{w(z)}\right) H_m\left(\frac{\sqrt{(}2)y}{w(z)}\right) \exp\left(-i\frac{k(x^2+y^2)}{2R(z)} - \frac{x^2+y^2}{w^2(z)}\right). \end{aligned} \tag{7}$$

Where P is the total beam power all parameters are defined as in [2]. To fully recreate a beam, each mode has a complex power scaled amplitude, a_{jnm} which describes the relative mode phases and amplitudes at the waist. These relative mode phases will differ as the beam propagates due to the Gouy phase.

In this model, a small shift or tilt in the cavity axis away from the input laser axis by a small addition of first order Hermite Gauss modes. Starting from the relations in Table 1 of [1] we can rearrange to obtain[1],

$$\Delta x(z) \approx \mathcal{R}_e\left(a_{10}(z)\right) w(z) \tag{8}$$
$$\Delta y(z) \approx \mathcal{R}_e\left(a_{01}(z)\right) w(z) \tag{9}$$
$$\theta^x(z) \approx \mathcal{I}_m\left(a_{10}(z)\right) \theta^x_{\text{div}} \tag{10}$$
$$\theta^y(z) \approx \mathcal{I}_m\left(a_{01}(z)\right) \theta^y_{\text{div}}. \tag{11}$$

4 Finesse Model

FINESSE is a frequency domain interferometer modelling software using the Hermite-Gauss mode basis[3]. The software outputs information via virtual detectors, of note is the non-physical amplitude detector (`ad`). The amplitude detector outputs the complex amplitude of the mode b_{jnm}. However, this complex amplitude also contains the plane wave phase, gouy phase, power and amplitude information. We can relate it to the usual a_{jnm} in equation 6 by multiplying though by the power and propagation terms in equation 7,

$$b_{jnm} = a_{jnm}\sqrt{P} \exp\left(i\left(n+m+1\right)\Psi(z)\right) \exp\left(i\left(\omega_j t - k_j z\right)\right). \tag{12}$$

[1] See section 4.4.2 of [5] for a recent derivation.

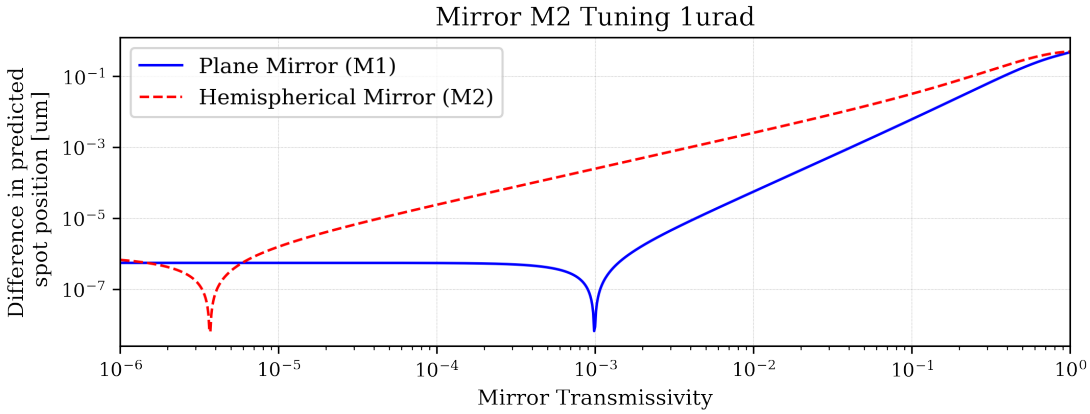

Figure 2: Difference geometric and modal model predictions of spot position as a function of mirror transitivity. The cavity was always impedance matched. One shortcoming of the geomtric model is that it does not take into account the transmissivity of the mirrors. For example, the geometric model incorrectly predicts a spot shift when the mirrors are totally transmissive. As illustrated above, this causes a small finesse-dependant mismatch between the models. In the high finesse case, a limiting mismatch may arise from either numerical precision, or, scattering into modes higher than first order (see approximations in the derivation of Eq. 8).

The complete field can then be described by these b_{jnm} parameters by

$$E(t,x,y,z) = \sum_j \sum_{nm} b_{jnm} \frac{u_{nm}(x,y,z)}{\exp\left(i\left(n+m+1\right)\Psi(z)\right)}. \tag{13}$$

To account for the inclusion of the rapidly rotating, $i(w_j t - k_j z)$, term in, b_{jnm}, which is common to all modes, we can find the inter-modal phase ϕ_{jnm}. Provided the input beam is in the fundamental mode and the cavity axis shift is small compared to the waist size of the beam we can work out the phase of the mode with respect the fundamental to subtract this term away,

$$\phi_{jnm} = Arg\left(b_{jnm}\right) - Arg\left(b_{j00}\right). \tag{14}$$

The cavity dynamics are also invariant to power and therefore we need to scale the mode amplitude by the power. Provided the amplitude of these modes are small, we can normalise by the absolute amplitude of the fundamental,

$$|a_{jnm}| = \frac{|b_{jnm}|}{|b_{j00}|}. \tag{15}$$

We can then substitute these into equations 8 to 11 to obtain

$$\Delta x_j = |a_{j10}|\, w(z) \cos\phi_{j10}, \tag{16}$$
$$\Delta y_j = |a_{j01}|\, w(z) \cos\phi_{j01}, \tag{17}$$
$$\theta^x_j = |a_{j10}|\, \theta^x_{\text{div}} \sin\phi_{j10}, \tag{18}$$
$$\theta^y_j = |a_{j01}|\, \theta^x_{\text{div}} \sin\phi_{j01}, \tag{19}$$

which is valid for an amplitude detector placed at any point in a cavity.

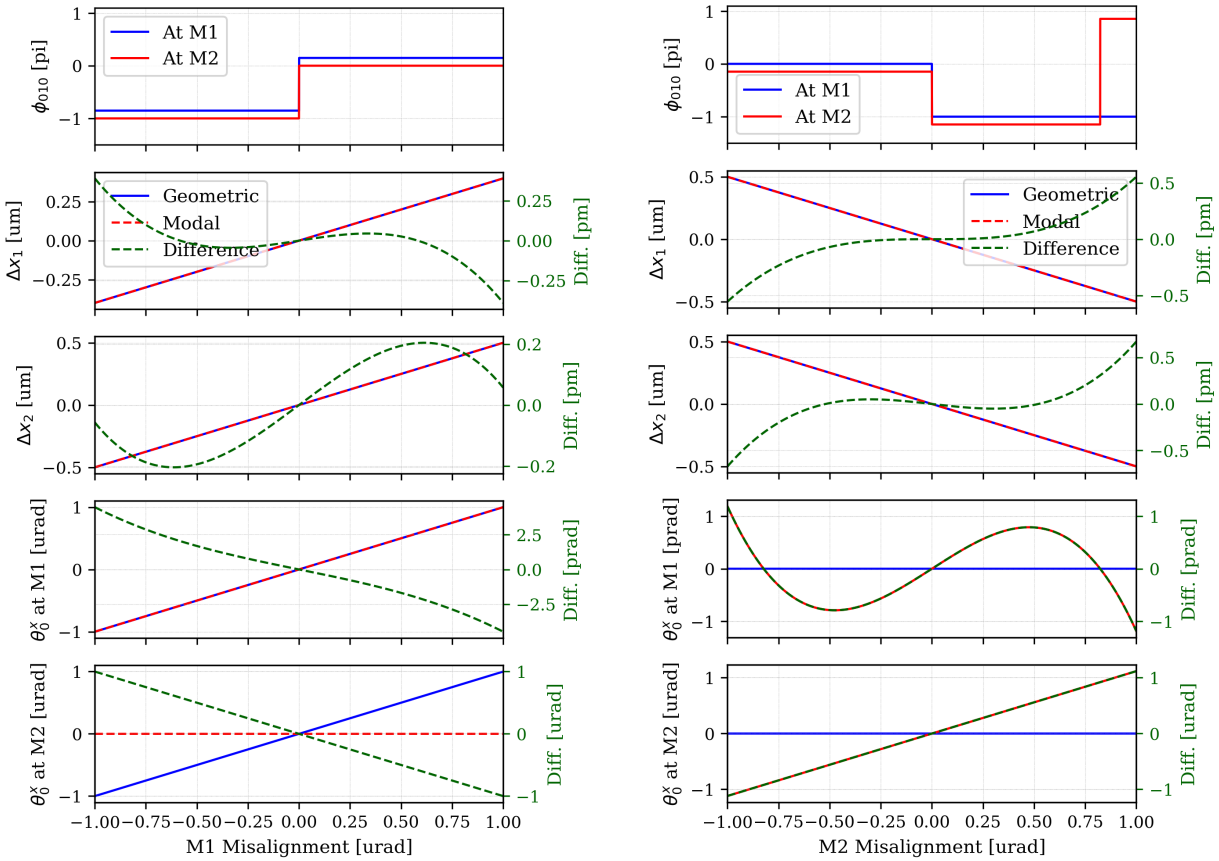

(a) Plane mirror rotated (M1)

(b) Hemispherical mirror rotated (M2)

Figure 3: The top plots shows the phase difference between the HG10 mode and the fundamental for the carrier light ($j = 0$, $n = 1$, $m = 0$). The second and third plots show the expected spot position shift on the plane mirror (M1, Δx_1) and the hemispherical mirror (M2, Δx_2) respectively, calculated using analytically using geometric optics (eq 3) and numerically using FINESSE modal model. The green trace shows difference (geometric - modal). The fourth and fifth plots show the wave-front tilt predicted by the Modal Model and the Geometric axis tilt, at M1 and M2 respectively.

5 Comparison

To verify the results above we checked the cavity dynamics predicted by FINESSE against the geometrical model for a hemispherical cavity. For this cavity we used an lossless impedance matched cavity with a mirror transmissivity of 1×10^{-6}. The mirror spacing was $0.1m$ and the end mirror radius of curvature was $0.5m$.

5.1 Spot Position Mismatches

As illustrated in Figure 3a and Figure 3b, numerically solving the modal model via FINESSE and equation 16 can be used to accurately predict the cavity axis shift throughout the cavity. However, cavity axis position calculated in equations 3 and 4 assumes an ideal infinite finesse cavity, any real cavity will experience losses which will shift the cavity axis. This causes a small, finesse dependant mismatch between the geometric results and the FINESSE modal model results as illustrated in figure 2.

5.2 Cavity Axis Mismatches

Equation 18 outputs the wave-front tilt. As stated in [1], at the waist this wave front tilt will coincide with the cavity axis tilt calculated geometrically. However, as is the case with the spot position, there will be a small difference caused by the inclusion of loss in the modal model. In our hemispherical cavity the waist is at the plane mirror (M1).

In the case of a small misalignment to a plane mirror then we expect from geometric considerations the cavity axis tilt to equal the mirror tilt. At M1, figure 3a shows an excellent agreement between the wave front tilt and cavity axis tilt. There is no waist at M2 and so the wave-front tilt must match the curved untitled surface of the hemispherical mirror in order to resonate and thus do not match the cavity axis tilt. This highlights an important constraint - the wave front tilt only matches the cavity axis tilt at the beam waist.

In the case of tilting the hemispherical mirror (figure 3b), geometrically we would expect no cavity axis tilt. The modal model shows a small wavefront tilt at the waist due to the inclusion of loss in this model, but otherwise excellent agreement. As before, at M2 the wave fronts match the curved tilted mirror surface as expected.

6 Conclusions

In the limit of a high finesse cavity, both numerically solving the modal model and geometric optics are able to predict the cavity spot position shift. However, as cavity finesse is reduced, the modal model is more accurate as it is able to model the losses.

One should be careful when interpreting the relations described in [1], as only at the waist is the wave front tilt equal to the cavity axis tilt. In a hemispherical cavity, the waist position is known and so either the modal model or geometric optics can calculate the cavity axis tilt. However, in general the waist position it is not known, in these cases the cavity axis tilt can be obtained by examining the spot positions output by the FINESSE and applying equation 5.

Acknowlegements

This work was predominatly carried out at the *Interferometer modeling and Finesse Workshop, August 2019*, which was supported by a Royal Society Wolfson Fellowship—jointly funded by the Royal Society and the Wolfson Foundation.

References

[1] Dana Z. Anderson. Alignment of resonant optical cavities. *Appl. Opt.*, 23(17):2944–2949, Sep 1984.

[2] Charlotte Bond, Daniel Brown, Andreas Freise, and Kenneth A. Strain. Interferometer techniques for gravitational-wave detection. *Living Reviews in Relativity*, 19(1):3, 2017.

[3] D Brown, R J E Smith, and A Freise. Fast simulation of gaussian-mode scattering for precision interferometry. *Journal of Optics*, 18(2):025604, 2016. http://arxiv.org/abs/1507.03806.

[4] Anthony E. Siegman. *Lasers*. University Science Books, 1986.

[5] H Wang. *Beware of Warped Surfaces: Near-Unstable Cavities for Future Gravitational Wave Detectors*. PhD thesis, University of Birmingham, 2017.